

EVINGCA: Adaptive Graph Clustering with Evolving Neighborhood Statistics

Randolph Wiredu-Aidoo

Abstract—Clustering algorithms often rely on restrictive assumptions: K-Means and Gaussian Mixtures presuppose convex, Gaussian-like clusters, while DBSCAN and HDBSCAN capture non-convexity but can be highly sensitive. I introduce EVINGCA (Evolving Variance-Informed Nonparametric Graph Construction Algorithm), a density-variance based clustering algorithm that treats cluster formation as an adaptive, evolving process on a nearest-neighbor graph. EVINGCA expands rooted graphs via breadth-first search, guided by continuously updated local distance and shape statistics, replacing fixed density thresholds with local statistical feedback. With spatial indexing, EVINGCA features log-linear complexity in the average case and exhibits competitive performance against baselines across a variety of synthetic, real-world, low-d, and high-d datasets.

I. INTRODUCTION

Clustering is central to unsupervised learning, yet classical algorithms face significant structural and scalability limits. Centroid-based methods such as K-Means [19] assume convex, linearly separable clusters, while density-based approaches like DBSCAN [8] or HDBSCAN [4], [21] often struggle under heterogeneous densities and are highly sensitive in higher dimensionality. Graph-based and deep clustering methods offer stronger performance but often demand heavy tuning or incur prohibitive computational cost.

I propose **EVINGCA** (Evolving Variance-Informed Nonparametric Graph Construction Algorithm), an alternative clustering paradigm that models cluster formation as an adaptive, evolving process on a nearest-neighbor graph. Instead of static density partitions, EVINGCA expands rooted graphs via breadth-first exploration guided by continuously updated local distance and shape statistics. This local statistical feedback replaces global parameters, enabling the method to adapt to heterogeneous densities and complex manifolds efficiently.

The main contributions of this work are:

- **Evolving statistical formulation:** clustering as an adaptive process governed by evolving neighborhood statistics rather than fixed density thresholds;
- **Multi-level nearest neighbor filters:** cluster growth is constrained by a density-variance based filter (called Level 1 or L1) and a local-shape-preservation filter (called Level 2 or L2), which operates based on per-dimension distances;

II. RELATED WORK

Clustering has been approached from several paradigms, each with characteristic strengths and weaknesses. I review the most relevant classes of methods to situate EVINGCA.

Centroid-based: Algorithms such as K-Means and its variants remain widely used due to their scalability and simplicity. However, their reliance on spherical cluster assumptions and the need to pre-specify k limit their flexibility in complex domains.

Density-based: DBSCAN detects arbitrarily shaped clusters and isolates noise points, but its reliance on global density thresholds causes failures under varying local densities. Extensions such as OPTICS [1] and HDBSCAN attempt to alleviate this through hierarchical density estimation and stability analysis, but these often increase algorithmic complexity and can still misrepresent fine-grained local structures.

Graph-based: Spectral clustering [24] leverages eigenstructure of similarity graphs to capture global manifolds, but requires constructing and decomposing dense affinity matrices, leading to $O(n^3)$ complexity and sensitivity to kernel choices. Community detection methods such as Louvain [3] and Leiden [26] avoid predefining k and scale better, yet suffer from the resolution limit problem, where small but meaningful clusters are merged.

Hierarchical: Linkage-based methods [17], [18] produce interpretable dendograms without committing to a fixed number of clusters. Nonetheless, their quadratic computational cost and sensitivity to the chosen linkage criterion restrict their usability for large datasets.

Model-based: Probabilistic approaches such as Gaussian Mixture Models [22] and Dirichlet Process Mixtures [9] offer statistical interpretability and uncertainty estimates. However, they assume specific parametric forms and deteriorate in high-dimensional spaces where likelihood surfaces become ill-conditioned.

Deep clustering: Recent methods couple representation learning with clustering objectives, including DEC [28],IMSAT [14], and DeepCluster [5]. While these approaches capture richer structures, they typically require heavy training pipelines, hyperparameter sensitivity, and are less interpretable compared to classical methods.

Positioning EVINGCA: EVINGCA is most closely related to density- and graph-based clustering. Like DBSCAN, it builds clusters from local neighborhoods, but instead of fixed global thresholds it employs evolving k -nearest-neighbor statistics that adapt to heterogeneous densities and gradients. Unlike spectral or community-detection methods, cluster growth proceeds through comparatively lightweight breadth-first expansion, visiting each point at most twice. With spatial indexing, this yields near-linear time complexity. By combining adaptive local feedback with graph-expansion simplicity, EVINGCA addresses the weaknesses of density-based clus-

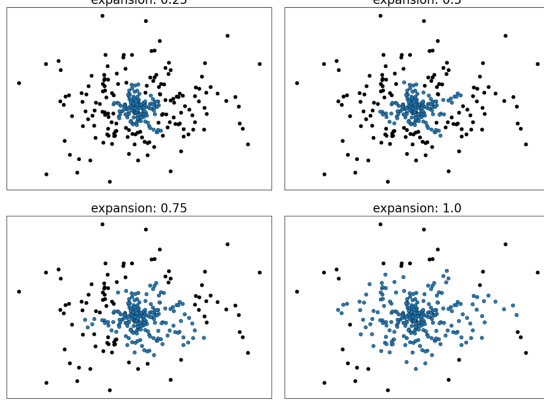


Fig. 1. Demonstration of the influence of expansion on a single Gaussian cluster. As expansion increases, the central cluster grows in size.

tering under heterogeneous conditions while remaining more scalable than heavy graph or deep-learning methods.

III. PRELIMINARIES

Let $X = \{x_i \in \mathbb{R}^d\}_{i=1}^n$ be a dataset and let $\|b - a\|$ be the Euclidean distance between points $a, b \in X$.

A. Evolving Neighborhood Statistics

EVINGCA maintains, for each growing cluster $C \subset X$, the running mean μ_C and the mean absolute deviation Δ_C of all observed k -NN distances since the instantiation of the cluster. These serve as proxies for local density and its variability:

$$\mu_C = \frac{1}{mk} \sum_{i=1}^m \sum_{j=1}^k d_{j,i}, \quad \Delta_C = \frac{1}{mk} \sum_{i=1}^m \sum_{j=1}^k |d_{j,i} - \mu_C|,$$

where $d_{j,i}$ is the distance to the j^{th} nearest neighbor for point i , and m is the current number of observed samples.

B. Level 1 (L1) Filter: Dynamic Distance Threshold

Traditional DBSCAN uses a fixed radius ε . EVINGCA replaces this with a variance-based tolerance: for any candidate b and existing cluster point a ,

$$\frac{\|b - a\| - \mu_C}{\Delta_C} > \epsilon \implies b \notin C.$$

If the standardized deviation exceeds ϵ (named `expansion` within the EVINGCA algorithm), b is excluded by the L1 filter.

C. Cluster Growth Order

To prevent dense cores from being absorbed by sparser regions, clusters expand in descending order of a density heuristic ($\approx \frac{k}{d_k}$), so that higher-density clusters claim neighbors first.

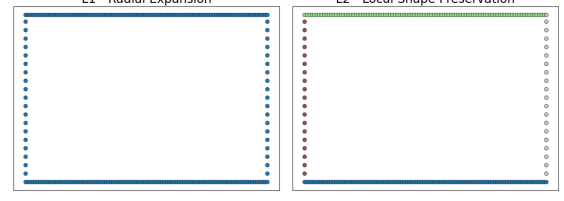


Fig. 2. Demonstration of L1 vs L2 on a rectangular point set. L1 fuses all points into one cluster while L2 preserves the linear shape of each side of the rectangle.

D. Level 2 (L2) Filter: Shape Preservation

a) *Shape acquisition*: EVINGCA enforces local shape coherence via a per-dimension compression descriptor. Around each cluster seed, it computes $\psi \in \mathbb{R}^d$, where

$$\psi[j] = \frac{1}{\binom{k+1}{2}} \sum_{i \in \ell} |X[\Phi_i, j] - X[\Phi_\ell, j]|,$$

with Φ being the indices of the seed and its k nearest neighbors. When considering a candidate b , it computes the dimensional differences between b and a neighbor in the cluster, forming a vector of the same length as ψ . If this vector does not exhibit a minimum similarity to ψ , b is excluded.

b) *Filter criterion*: Given a candidate point b and a reference neighbor a within an existing cluster, let

$$p_j(b, a) = \frac{|X[b, j] - X[a, j]|}{\sum_{\ell=1}^d |X[b, \ell] - X[a, \ell]|},$$

$$w_j = \frac{\psi[j]}{\sum_{\ell=1}^d \psi[\ell]}$$

The vector $p(b, a) = (p_1, \dots, p_d)$ represents the *relative pattern* of differences between b and a , while w encodes the pattern within the core of the reference neighbor's cluster. The Level-2 filter accepts b if

$$p(b, a) \approx w$$

in the sense that all coordinates satisfy

$$|p_j(b, a) - w_j| \leq \tau, \quad j = 1, \dots, d,$$

for a tolerance parameter $\tau \geq 0$.

E. Small Cluster Management

a) *Fragmented Distributions*: The clustering process may generate a fragmented distribution with several clusters that are too small to be considered significant. Such clusters can be treated as uncertain and their points can be labeled as new data, to be assigned to a larger, more significant class.

b) *Assignment rule*: Let x be a point to assign (either from a small cluster or an unseen sample), and $\mathcal{N}_k(x)$ its k -nearest neighbors. For each cluster label c , define

$$\mathcal{N}_k^{(c)}(x) = \{x_i \in \mathcal{N}_k(x) : y_i = c\}, \quad u_i = \frac{x_i - x}{\|x_i - x\|},$$

the angular isotropy score:

$$I_c = |\mathcal{N}_k^{(c)}(x)| - \left\| \sum_{x_i \in \mathcal{N}_k^{(c)}(x)} u_i \right\|,$$

and the cluster score:

$$S_c = \frac{I_c}{\min_{x_i \in \mathcal{N}_k^{(c)}(x)} \|x_i - x\|},$$

to account for the nearness of competing clusters. Then assign:

$$c^* = \arg \max_c S_c.$$

This favors the cluster whose neighbors are abundant, surround x , and are likely near to it, promoting coherent boundaries and preventing attachment to distant, one-sided clusters due to mere k-NN majority vote. The distance to the nearest cluster neighbor is used for visual coherence – angular isotropy loses relevance as the nearness of the nearest cluster neighbor dominates.

F. Heuristic Modulators

As with many existing density-based methods, directly tuning parameters can be a sensitive process as the scale of distance between points can be extremely small. To mitigate this effect, and to guide EVINGCA towards stable, visually coherent clusterings, a set of mathematical heuristics was developed and validated against a set of developmental datasets (Appendix B). These heuristics, dubbed h_1, \dots, h_4 within Algorithm 1, are empirical tweaks that were found to improve efficiency, reduce tuning sensitivity, and moderate cluster growth in a more visually agreeable manner, even at default values for all parameters.

The heuristics are embedded throughout the clustering process, performing a variety of functions such as:

- Rescaling distances for usage in downstream computations;
- Modulating cluster expansion through modifications to L1 and L2;
- Modifying the small cluster reassignment process to prevent extreme outliers from joining significant clusters;

With these definitions in place, I now present the full algorithm.

IV. PROPOSED METHOD

EVINGCA performs clustering via an adaptive, density-ordered graph expansion. It first selects high-density seeds, then iteratively grows each cluster in breadth-first order, applying two levels of local filters (L1/L2) based on evolving neighborhood statistics and shape descriptors. Finally, small clusters are deconstructed and their points assigned to larger nearby clusters.

Algorithm 1 EVINGCA($X; \ell, e, b, m, M, P$)

Require: Dataset $X = \{x_i \in \mathbb{R}^d\}_{i=1}^n$; level $\ell \in \{1, 2\}$; expansion $e \in [0, 1]$; blur $b \in [0, 1]$; max-neighbors $m \in \mathbb{N}$; min-cluster-size $M \in \mathbb{N}$; small-cluster-policy $P \in \{\text{“Reassign”, “Noise”}\}$

Initialization

- 1: $s \leftarrow \sum_{j=1}^d (\max X[:, j] - \min X[:, j])^2$
- 2: $\mathcal{I} \leftarrow \text{SPATIALINDEX}(X)$
- 3: $D[i] \leftarrow \text{DENSITYHEURISTIC}(\mathcal{I}, X[i], b, s)$
- 4: priority queue $U \leftarrow$ indices sorted by D (descending)
- 5: $L[i] \leftarrow \text{UNVISITED}$ for all i

Cluster growth

- 6: $c \leftarrow 0$
- 7: **while** U not empty **do**
- 8: FIFO queue $Q \leftarrow [\text{pop}(U)]$
- 9: $\mu_C \leftarrow 0, \Delta_C \leftarrow 1, n \leftarrow 0$
- 10: **if** $\ell = 2$ **then**
- 11: $\psi \leftarrow \text{SHAPEDESCRIPATOR}(X[Q.\text{front}])$
- 12: **while** Q not empty **do**
- 13: $i \leftarrow \text{pop}(Q)$
- 14: $L[i] \leftarrow c, n \leftarrow n + 1$
- 15: $(\Phi, \delta) \leftarrow \mathcal{I}.\text{QUERY}(i, m + 1)$
- 16: $(\Phi, \delta) \leftarrow \{(\Phi_j, \delta_j) : L[\Phi_j] = \text{UNVISITED}\}$
- 17: // L1 filter
- 18: remove Φ_j if $h_1((\delta_j - \mu_C)/\Delta_C, b) > h_2(e, D[i])$
- 19: // L2 filter
- 20: **if** $\ell = 2$ **then**
- 21: **if** $\max_{l=1..d} h_3(|p_l(\Phi_j, i) - w_l|) > \tau$ **then**
- 22: reject Φ_j
- 23: // update Δ_C
- 24: $\Delta_C \leftarrow \frac{\Delta_C(n - 1 + |Q|) + \sum |\delta_j - \mu_C|}{n - 1 + |Q| + |\Phi|}$
- 25: // update μ_C
- 26: $\mu_C \leftarrow \frac{\mu_C(n - 1 + |Q|) + \sum \delta_j}{n - 1 + |Q| + |\Phi|}$
- 27: // add to the frontier
- 28: **for all** $j \in \Phi$ **do**
- 29: enqueue j into Q ; remove j from U
- 30: $L[j] \leftarrow \text{FRONTIER}$
- 31: $c \leftarrow c + 1$

Small-cluster refinement

- 32: **if** $P = \text{“Reassign”}$ **then**
- 33: Dismantle and reassign clusters of a size below M with nearest neighbor distance threshold $h_4(s, d)$.
- 34: **else**
- 35: Assign all points in clusters of a size below M to noise.
- 36: **return** L

A. Overview

- 1) **Preprocessing:** EVINGCA was developed primarily using minmax-scaled data. Before clustering, datasets were typically scaled such that all features were in $[0, 1]$. While it is not dysfunctional under other forms of scaling, its heuristics and components best exhibit their intended behavior in this regime.

2) **Parameters:**

a) **level:**

- Selects the level for clustering, L1 (density-variance based clustering) or L2 (L1 clustering + shape awareness).

b) **expansion:**

- A value in $[0, 1]$ controlling cluster size by increasing density variance tolerance. At 0, nearly every point forms its own cluster; as it approaches 1, clusters become larger and sparser (though not necessarily a single cluster). Its default value is 0.5.

c) **blur:**

- Like expansion, this parameter is a value in $[0, 1]$ affecting cluster granularity. During density measurement (DensityHeuristic), blur is used to clip k-NN distances to a minimum value relative to the full dataset scale, s . It is also lightly incorporated into the L1 filter (via heuristics) to facilitate a more controllable expansion process – maximal blur effectively removes all variance in measured densities and disables L1 filtering, allowing full expansion across the k-NN graph. Its default value is 0.5.

d) **max_neighbors:**

- The number of neighbors fetched for each point. A greater number of neighbors results in larger clusters on average. This is especially helpful for highly dense, interconnected regions. Its default value is dataset dependent.

e) **min_cluster_size:**

- The minimum size of a cluster below which it is reassigned. Its default value is dataset dependent.

f) **small_cluster_policy:**

- The policy controlling the manner in which clusters below **min_cluster_size** in size are handled. By default, points in such clusters can be reassigned to nearby larger clusters. However, it remains an option to simply assign them to a collective noise cluster.

3) **Seed Selection:** Compute a density heuristic $D[i]$ for each point i . Then sort points by D descending, and initialize all as unvisited.

4) **Density-Ordered Expansion:**

- Pop the highest-density unvisited point p to start a new cluster C .
- Maintain a running mean and deviation (μ_C and Δ_C) of the k-NN distances observed so far in C .
- Expand C breadth-first, filtering neighbors by L1 and optionally, L2.
- Update μ_C and Δ_C incrementally after accepting new neighbors.

5) **Small-Cluster Refinement:** With a “Reassign” policy, clusters with size $< M$ have each of their points reassigned to a different cluster from among their k-nearest neighbors. Neighbors are restricted to those

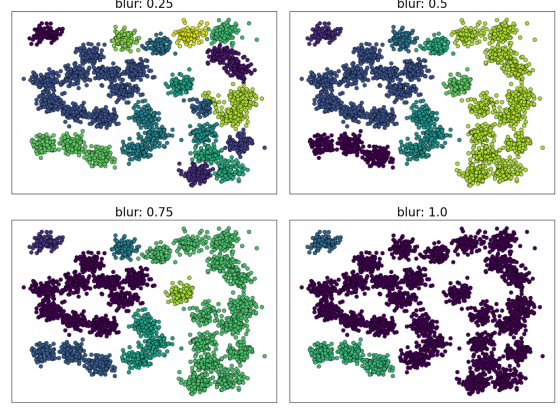


Fig. 3. Demonstration of the effect of **blur** on the D31 dataset. Clusters grow more aggressively with higher values of blur, as its maximal value disables L1 filtering entirely.

within a certain distance threshold, governed by h_4 . With a “Noise” policy, small clusters are simply fused into a collective noise cluster.

B. Time Complexity

Let N be the number of data points, d the dimensionality, and c the number of neighbors retrieved per k-NN query. During EVINGCA’s expansion and refinement phases, each point performs one or more neighborhood queries to guide local density-based growth. To maintain sufficient connectivity while keeping computation tractable, c typically scales as $O(\min(\max_{\text{neighbors}}, \log N))$. Treating **max_neighbors** as a constant, we have $c = O(\log N)$ in the practical regime.

Let $C_{nn}(N, d, c)$ denote the cost of retrieving c nearest neighbors for one query in d dimensions. This cost depends on the indexing method used: for example, $C_{nn} = O(dN)$ for brute-force search and $C_{nn} = O(d \log N)$ for efficient spatial structures such as trees or graph-based indexes.

Beyond neighbor retrieval, EVINGCA performs local computations for each point, including: (i) density and variance estimation over its c neighbors, (ii) local shape estimation, and (iii) optional refinement or merging of clusters. Each of these operations scales linearly with the number of neighbors and potentially with dimensionality, contributing an additional $O(dc)$ cost per point.

Hence, the total per-point cost is:

$$O(C_{nn}(N, d, c) + dc),$$

and across all points:

$$O(N \cdot (C_{nn}(N, d, c) + dc)).$$

If an efficient sublinear neighbor-retrieval scheme is used (e.g., $C_{nn} = O(d \log N)$) and $c = O(\log N)$, the total complexity becomes:

$$O(N d \log N).$$

C. Space Complexity

EVINGCA maintains a neighborhood graph that stores the c nearest neighbors for each of the N points. This structure supports efficient local expansions and is constructed once at initialization, after which it is reused throughout the algorithm. Let d denote the data dimensionality and c the number of stored neighbors per point.

The neighborhood graph requires $O(Nc)$ storage, while the input data matrix contributes $O(Nd)$. Additional bookkeeping structures (cluster labels, density values, and temporary buffers) are linear in N and therefore do not alter the asymptotic order. Thus, the overall space complexity is

$$O(Nd + Nc) = O(N(d + c)).$$

Under the common practical assumption that $c = O(\log N)$ (Section IV-B), the resulting complexity simplifies to

$$O(N(d + \log N)).$$

V. TERMINOLOGY

Throughout this paper, I use the term **connectivity** to refer to the combination of (a) **high proximity** between clusters and (b) **flat or gradual density gradients** across cluster boundaries. High connectivity implies that inter-cluster boundaries are not easily distinguishable using local distance or density estimates, making it difficult for density-based methods to reliably separate clusters without over or under-segmentation.

VI. EXPRESSIVE CAPACITY

A. Purpose

To identify data distributions where EVINGCA intrinsically excels or fails, I use a ground-truth-guided benchmark: Adjusted Rand Index (ARI) with true labels selects the strongest hyperparameter configuration per dataset. This inflates performance and is not a proxy for real-world deployability, but it removes confounds such as tuner quality or sub-sampling stability from the assessment of algorithmic capability. For context, EVINGCA is evaluated alongside standard clustering algorithms, whose design and performance serve as diagnostic baselines.

B. Datasets

I evaluate across synthetic and real-world datasets spanning 2–2000 dimensions.

2–3D datasets: Synthetic benchmarks include *Compound*, *Spiral*, *Flame*, *Labirynth*, *D31*, *Nested Circles*, *Smile*, *Mk3*, *Mk4*, and *Tetra*, plus the real-world *Fish* dataset [11], [13], [25].

4D+ datasets: From UCI [7], I include *Iris*, *Banknote*, *Ecoli*, *Seeds*, *Wine*, *Pendigits*, *Statlog*, and *WDBC*. I also use *Digits* [23], *USPS* [15], [2], human activity recognition – training subset (*HAR Train Subset*) [27], *Fashion-MNIST* [11], and the text corpus *20 Newsgroups* (2000D TF-IDF embedding) [23]. Two Gaussian mixtures, *G2mg_128_20*, and *G2mg_128_30* [11], probe the interplay of dimensionality and connectivity.

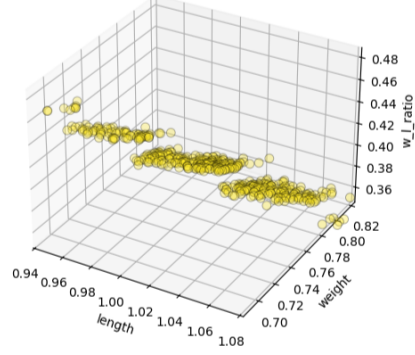


Fig. 4. A 3D plot of a cluster in the Fish dataset. This cluster, similar to others, is composed of flattened x-y sheets, biasing EVINGCA towards over-segmentation.

C. Algorithm Implementations

EVINGCA is implemented primarily in Python. For speed, it utilizes approximate nearest neighbors (via an HNSW [20]) as well as vectorized operations with the Numpy library [12]. For other baselines, I use HDBSCAN (v0.8.40), K-means, Spectral Clustering, and Gaussian Mixture Models (GMM), implemented in Scikit-Learn v1.6.1.

D. Evaluation Metrics

I report:

- **ARI**: agreement with ground truth.
- **Runtime**: execution time (s), excluding preprocessing.
- **Normalized Mutual Information (NMI)**: reported in Appendix A.

E. Experimental Protocol

All datasets were shuffled (seed 42) and minmax scaled to $[0, 1]$. To limit runtimes, tuning was capped at **120s per dataset**, with best-so-far configurations returned if exceeded. Datasets above 10k samples were sub-sampled uniformly to 10k points. No dimensionality reduction was applied.

Each algorithm was tuned over up to 51 random configurations over algorithm-specific parameter ranges. For K-means, Spectral, and GMM, the true number of clusters was provided; density-based methods (HDBSCAN, EVINGCA) used the first trial to assess the default configuration and used the remaining 50 to explore their full parameter space. For all methods, the selected hyperparameter configuration was that which achieved the highest ARI with respect to ground truth. All configurations were then rerun 10 times. Implementations involving stochasticity (K-means, GMM, Spectral, EVINGCA) received a different random seed for each run, while HDBSCAN was rerun primarily to capture runtime variance.

Experiments ran on an Intel i7 (12 cores, 2.10 GHz) with 16 GB RAM; multi-core support was enabled (`n_jobs = -1`).

Full per-dataset results and NMI are in Appendix A; main text reports ARI and runtime.

TABLE I

GROUND-TRUTH-TUNED CLUSTERING PERFORMANCE (ARI \pm 1 SD) ACROSS DATASETS; SD < 0.005 ARE OMITTED. DEVELOPMENT DATASETS ARE MARKED WITH *. BOLD INDICATES THE BEST ARI PER ROW.

Dataset (N, D)	EVINGCA	HDBSCAN	K-means	GMM	Spectral
<i>2-3D datasets</i>					
Spiral (312, 2)	1.00	1.00	-0.01	0.02 \pm 0.01	0.80
Smile (1000, 2)	1.00	1.00	0.52 \pm 0.07	0.65 \pm 0.15	0.32 \pm 0.08
Labirynth (3546, 2)	0.76	0.55	0.30 \pm 0.02	0.55 \pm 0.09	0.72
Fish* (4080, 3)	0.80	0.86	0.81	0.84	0.75 \pm 0.09
D31 (3100, 2)	0.92	0.61	0.92 \pm 0.02	0.92 \pm 0.02	0.95
<i>4D+ datasets</i>					
Ecoli (336, 7)	0.72	0.44	0.43 \pm 0.05	0.62 \pm 0.01	0.39
Pendigits (10000, 16)	0.78	0.54	0.55 \pm 0.04	0.55 \pm 0.03	0.74
Digits (1797, 64)	0.87	0.40	0.64 \pm 0.04	0.64 \pm 0.02	0.81
USPS (9298, 256)	0.61	0.11	0.53 \pm 0.02	0.00	0.65
G2mg_128_30 (2048, 128)	0.08	0.00	0.95	0.95	0.93

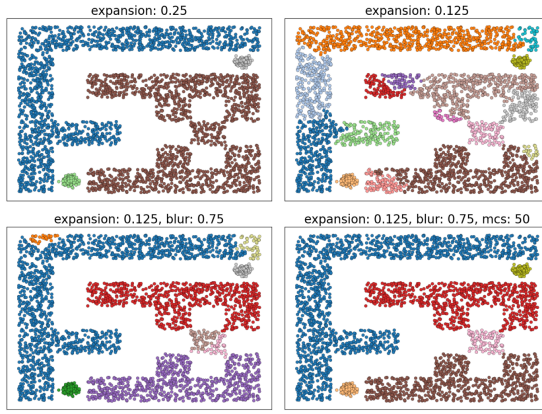


Fig. 5. Demonstration of the interactive effects of EVINGCA’s parameters on *Labirynth*. Tuning individual parameters can be sensitive, but binary-search-like adjustments combined with small cluster clean-up via `min_cluster_size` (mcs) can create desired clusters. The final configuration (bottom right) achieves an ARI of 0.999 with ground truth.

F. Behavioral Analysis

EVINGCA clusters by expanding along density gradients, which makes it highly effective on irregular structures (*Spiral*, *Smile*, *Nested Circles*; ARI ≈ 1.0). When smooth gradients connect otherwise distinct clusters, however, it can under-segment: in *Labirynth*, inter-cluster connections bias it toward merging clusters (0.76 ARI under budget), though more principled tuning can fully recover labels (Fig. 5). Similarly, convex datasets with sharp gradients or dense cores (*D31*, *Tetra*) are recovered well (≈ 0.9 –1.0 ARI), while smoother transitions (*Mk3*, *Seeds*) lead to moderate under-segmentation compared to centroid-based methods.

Another challenge appears when clusters contain internal valleys. In *Fish*, intra-cluster sheets or strips induce mild over-segmentation (0.80 ARI vs. 0.86 for HDBSCAN). This case also highlights the role of L2 expansion: the x–y substructure encourages additional splits to preserve z-axis compression (Fig. 4), though ground-truth tuning mitigates this by selecting L1.

High dimensions reduce variance in distances, resulting in smoother gradients and greater apparent connectivity. When

paired with moderate intrinsic connectivity between clusters, it can cause collapse. I observe this from EVINGCA’s performance on datasets at or above 128 dimensions:

First, there is the case of *G2mg_128_30*, where EVINGCA achieves only 0.08 ARI. This dataset features 2 Gaussian clusters with high proximity and moderately smooth gradients between them, as seen from 3-dimensional PCA-embeddings. When reduced to 3D, EVINGCA achieves 0.93 ARI under the same experiment. At the same time, EVINGCA achieves even stronger performance (0.99 ARI) on *G2mg_128_20* without dimensionality reduction. This dataset is a modified version of *G2mg_128_30* with greater separation between the two Gaussian clusters, creating a steeper density gradient between them. This allows EVINGCA to latch onto gradient structure and appropriately separate the clusters.

In even greater dimensionality, performance remains beyond that of *G2mg_128_30*. EVINGCA attains 0.61 ARI on *USPS* (256D), 0.52 on *HAR* (562D), and 0.38 on *Fashion-MNIST* (784D). These results, along with findings in lower dimensionality, indicate dimensionality is not the sole cause of collapse. Rather, apparent connectivity, whether intrinsic or amplified by dimensionality, is the primary failure mode for EVINGCA.

Extreme sparsity, as in *20 Newsgroups* (2000D), erases gradients entirely, causing universal failure (ARI ≈ 0). In such cases, recovery of any structure becomes impractical for baselines as the curse of dimensionality and intrinsic sparsity removes discernible structure.

G. Anytime Performance

Beyond final performance, it is also instructive to examine how clustering quality evolves as parameters are explored. In this setting, each trial records the best ARI achieved up to that point, yielding an *anytime curve*. EVINGCA was evaluated under a uniform 51-trial parameter search on each dataset, enabling consistent comparison across datasets.

On average, EVINGCA improves rapidly: from an initial mean ARI of 0.43 at trial 1, it crosses a “moderate” threshold of 0.6 by trial 9 and exceeds 0.7 by trial 25. After this point, gains become modest. The curve meets a relative plateau criterion (remaining improvement ≤ 0.05 ARI), though the local slope analysis suggests that performance is still drifting

TABLE II

RUNTIMES (MEANS \pm 1 SD) ACROSS DATASETS UNDER GROUND-TRUTH-TUNED CONFIGURATIONS. STANDARD DEVIATIONS < 0.005 s ARE OMITTED. DEVELOPMENT DATASETS ARE MARKED WITH *. BOLD INDICATES THE BEST PER ROW.

Dataset (N, D)	EVINGCA	HDBSCAN	K-means	GMM	Spectral
Spiral (312, 2)	0.02 s	< 0.01 s	0.01 s	0.01 s	0.11 s
Labirynth (3546, 2)	0.20 s	0.04 s	0.01 s	0.45 s	0.54 s
Fish* (4080, 3)	0.13 s	0.06 s	0.01 s	0.07 s	0.51 s
Pendigits (10000, 16)	0.39 s	1.08 s	0.02 s	0.45 s	4.06 s
Digits (1797, 64)	0.08 s	0.16 s	0.01 s	0.14 s	0.29 s
G2mg_128_30 (2048, 128)	0.12 s	0.41 s	0.01 s	0.09 s	0.86 s
USPS (9298, 256)	0.74 s	16.29 s	0.09 s	0.22 s	4.11 s
HAR Train Subset (7352, 562)	0.76 s	25.60 s	0.12 s	78.83 s	4.64 s
Fashion-MNIST (10000, 784)	2.10 s	62.55 s	0.30 s	0.86 s	3.61 s
20 Newsgroups (10000, 2000)	2.64 s	159.40 s	1.08 s	4.56 s	3.78 s

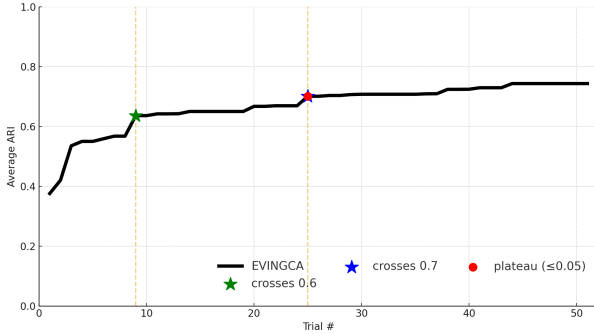


Fig. 6. Average anytime performance of EVINGCA across non-development datasets. The curve shows the mean best ARI as a function of parameter trials. EVINGCA improves rapidly, crossing 0.7 before starting to plateau (remaining improvement ≤ 0.05 ARI units) near that level.

upward at a very low rate. Thus, EVINGCA shows signs of plateauing near 0.7, but has not fully settled by the end of the 51 trials. The final average ARI is approximately 0.77.

This trajectory highlights EVINGCA’s strong anytime behavior: it reaches useful quality quickly, achieves robust performance well before exhausting its trial budget, yet continues to slowly improve with subsequent tuning.

H. Stability Analysis

Stability was evaluated in terms of standard deviation in ARI score across different initializations via random seed. Note that while EVINGCA itself is deterministic, its use of an HNSW index for neighborhood estimation injects stochasticity into the final label output.

Across all datasets, EVINGCA maintains low variability ($\sigma_{ARI} < 0.005$) even under stochastic neighbor graphs, suggesting robustness to approximate k NN noise. In contrast, K-means, GMM, and Spectral clustering show greater instability due to random initialization or eigendecomposition, though most deviations remain small.

Ultimately, EVINGCA’s stability supports the design choice to use HNSW: Individual errors or variance in nearest neighbors are effectively neutralized by reliance on broader nearest-neighbor distance statistics, granting EVINGCA robustness to the use of approximate spatial indexing.

I. Runtime Analysis

Runtime was measured as wall-clock time (s) per dataset, excluding preprocessing and I/O. All experiments were conducted on an Intel i7 (12 cores, 2.10 GHz, 16 GB RAM) with multi-threaded execution ($n_jobs=-1$). Values represent averages over ten runs with ground-truth-tuned configurations.

a) Scaling with sample size (N): For small datasets ($N < 5 \times 10^3$), EVINGCA completes within 0.1–0.2 s, showing approximately linear growth with N . Between the Spiral (312 points, 0.02 s) and Labirynth (3546 points, 0.20 s) datasets, the runtime increases roughly 10× for an 11× increase in N , consistent with the expected $O(N \log N)$ scaling. At $N = 10^4$, runtimes remain below 0.5 s for moderate dimensions (e.g., Pendigits, 16D), confirming the near-linear trend predicted by Section IV-B.

b) Scaling with dimensionality (D): Holding N roughly constant, runtime increases sublinearly with D . From Pendigits (16D, 0.39 s) to USPS (256D, 0.74 s) and Fashion-MNIST (784D, 2.10 s), the runtime grows by approximately 5× for a 50× increase in D , indicating a sublinear relationship. Even in high-dimensional settings such as 20 Newsgroups (2000D, 2.64 s), EVINGCA remains tractable, aided by vectorized distance computations and approximate nearest-neighbor search (HNSW indexing).

c) Comparison with baselines: EVINGCA consistently ranks between centroid-based methods (K-means, GMM) and graph- or density-based algorithms (HDBSCAN, Spectral) in raw speed. Across the ten datasets shown in Table II:

- EVINGCA is typically 2–5× slower than K-means but 10–50× faster than HDBSCAN and Spectral clustering.
- On medium-size datasets (5k–10k samples, $D \leq 100$), EVINGCA averages ≈ 0.4 s versus ≈ 1 s for HDBSCAN and > 3 s for Spectral.
- In high-dimensional cases ($D \geq 500$), EVINGCA outperforms HDBSCAN by one to two orders of magnitude (e.g., 0.76 s vs. 25.6 s on HAR, 2.1 s vs. 62.6 s on Fashion-MNIST).

K-means remains the absolute fastest method due to its minimal per-iteration cost and absence of neighbor queries, but EVINGCA achieves significantly greater expressivity with only a modest runtime penalty.

TABLE III

EXPRESSIVE CAPACITY ABLATION (ARI \pm 1 SD) ACROSS DATASETS; SD < 0.005 ARE OMITTED. DEVELOPMENT DATASETS ARE SUFFIXED WITH *. BOLD INDICATES THE BEST VALUE PER ROW.

Dataset (N, D)	Minmax Scaler	Standard Scaler	No Scaler	SCP = Noise	Random Seeding	No Heuristics
<i>2-3D datasets</i>						
Spiral (312, 2)	1.00	1.00	1.00	1.00	1.00	1.00
Smile (1000, 2)	1.00	1.00	0.98 ± 0.06	1.00	1.00	0.99
Labirynth (3546, 2)	0.76	0.76	0.76	0.76	0.76	0.97
Fish* (4080, 3)	0.80	0.76	0.87	0.80	0.69	0.80
D31 (3100, 2)	0.92	0.89	0.92	0.62	0.85	0.83
<i>4D+ datasets</i>						
Ecoli (336, 7)	0.72	0.60	0.69	0.47	0.46	0.69
Digits (1797, 64)	0.87	0.76	0.83	0.71	0.84	0.81
G2mg_128_30 (2048, 128)	0.08	0.05 ± 0.02	0.07 ± 0.01	0.02 ± 0.01	0.02	0.01 ± 0.01
USPS (9298, 256)	0.61	0.53	0.61	0.34	0.50	0.55
HAR Train Subset (7352, 562)	0.52	0.53	0.29	0.32	0.51	0.45

VII. ABLATION STUDY

A. Experimental Setup

To assess the contribution of EVINGCA’s design choices, I conduct ablation experiments over key aspects of the algorithm. Four factors are ablated: (1) normalization strategy (min–max, standard, or none), (2) small-cluster policy (reassignment vs. labeling as noise), (3) cluster seeding (ordered vs. random), and (4) heuristics (enabled vs. disabled). ARI is the primary evaluation metric, averaged over ten runs. Results are reported in Table VI. Development datasets are excluded when assessing significance.

B. Results Summary

Wilcoxon Signed Rank tests with Holm–Bonferroni correction on the baseline vs each ablation reveal three components as statistically significant:

- **Small-cluster policy:** Setting the small-cluster policy to “Noise” instead of “Reassign” significantly reduces ARI, with the strongest degradations in higher-dimensional datasets (e.g., Digits $0.87 \rightarrow 0.71$, HAR $0.52 \rightarrow 0.32$).
- **Seeding:** Random initialization consistently underperforms ordered seeding, confirming that deterministic initialization improves both stability and reproducibility.
- **Heuristics:** Removing heuristics lowers ARI overall, though some datasets (e.g., Labirynth $0.76 \rightarrow 0.97$) benefit when constraints and modifications are relaxed.

Normalization ablations under expressive capacity do not reach significance after Holm–Bonferroni correction. Relative to Minmax Scaling, Standard Scaling and no scaling were observed to provide similar upper bound performance.

C. Interpretation

The ablation confirms that EVINGCA’s core design choices. Robust handling of small clusters, deterministic seeding, and heuristic constraint enforcement are decisive under expressive capacity, where algorithmic potential is isolated. Heuristics contribute meaningfully to clustering quality overall, though their removal can occasionally improve results on specific geometric datasets. Normalization effects appear secondary but dataset-dependent, positioning it as a potential direction of optimization.

VIII. CONCLUSION

This work introduced **EVINGCA**, a density-variance based, shape-aware clustering algorithm that models cluster formation as an adaptive, locally guided expansion process. Through an *expressive capacity* analysis conducted under with ground-truth guidance, we isolated EVINGCA’s intrinsic representational ability independent of tuner quality or subsampling stability. This framework provided an empirical estimate of upper-bound capability under constrained exploration, revealing both the strengths and structured sensitivities of the method.

Across synthetic and real-world benchmarks spanning 2–2000 dimensions, EVINGCA achieved near-perfect recovery on irregular, non-convex manifolds and competitive accuracy on convex or moderately overlapping datasets. Its principal failure modes, including under-segmentation in smoothly connected manifolds and reduced contrast in high-dimensional regimes, reflect predictable sensitivity to gradient smoothness and connectivity rather than stochastic instability. In these cases, performance degradation remains bounded and interpretable. Stability analyses confirmed low variance across approximate k NN initializations, demonstrating robustness to neighbor estimation noise. Runtime evaluations further showed that EVINGCA maintains practical computational cost, typically between centroid-based and graph-based baselines, and scales sublinearly with dimensionality through approximate indexing and an efficient expansion algorithm.

Under a modest ground-truth-guided search of 51 parameter configurations per dataset, EVINGCA performed competitively or better than baselines that received the true number of clusters. This indicates that high-quality regions in its five-parameter space are relatively dense and accessible, suggesting that strong performance arises from coherent parameter interactions rather than tuning luck. The observed anytime behavior, characterized by rapid early improvement followed by gradual convergence, further supports this interpretation, showing that EVINGCA reaches useful quality quickly while continuing to refine with additional exploration.

Together, these findings characterize EVINGCA’s empirical expressive capacity: a stable, geometrically adaptive clustering process capable of representing diverse structural regimes with

competitive efficiency and robustness across a broad range of conditions.

IX. FUTURE WORK

I outline several directions to strengthen **EVINGCA** and broaden its applicability.

- **Unsupervised experimentation and self-tuning:** Extend the current ground-truth-based analysis to fully unsupervised settings. Develop parameter selection schemes that can identify reliable configurations without ground-truth labels. Integrate these into a unified tuning pipeline capable of balancing clustering quality and computational cost across datasets.
- **Adaptive preprocessing and diagnostics:** Implement automatic triggers for dimensionality reduction (e.g., PCA or random projections) when distance variance collapses. Add connectivity and density-contrast diagnostics to adapt neighborhood sizes and merging strategies on the fly.
- **Runtime and scalability:** Although EVINGCA attains practical runtimes through approximate neighbor indexing and vectorized computation, further efficiency could be realized by migrating core iterative routines to compiled backends such as C or C++. Alternatively, parallelization schemes leveraging multi-threaded or GPU execution could further accelerate large-scale runs without altering algorithmic behavior. Evaluating these approaches would clarify how much of EVINGCA’s current runtime stems from Python-level overhead versus inherent algorithmic cost, and define its scalability envelope for higher-volume or real-time applications.

REFERENCES

- [1] Mihael Ankerst, Markus M. Breunig, Hans-Peter Kriegel, and Jörg Sander. Optics: Ordering points to identify the clustering structure. In *Proceedings of the 1999 ACM SIGMOD International Conference on Management of Data*, pages 49–60. ACM, 1999.
- [2] Bistaumanga. Usps dataset. <https://www.kaggle.com/datasets/bistaumanga/usps-dataset>, 2018. Accessed: 2025-10-26. Based on the original dataset by Hull (1994).
- [3] Vincent D. Blondel, Jean-Loup Guillaume, Renaud Lambiotte, and Etienne Lefebvre. Fast unfolding of communities in large networks. *Journal of Statistical Mechanics: Theory and Experiment*, 2008(10):P10008, 2008.
- [4] Ricardo J. G. B. Campello, Davoud Moulavi, and Jörg Sander. Density-based clustering based on hierarchical density estimates. In *Proceedings of the Pacific-Asia Conference on Knowledge Discovery and Data Mining*, pages 160–172. Springer, 2013.
- [5] Mathilde Caron, Piotr Bojanowski, Armand Joulin, and Matthijs Douze. Deep clustering for unsupervised learning of visual features. In *Proceedings of the European Conference on Computer Vision (ECCV)*, pages 132–149, 2018.
- [6] H. Chang and D. Y. Yeung. Robust path-based spectral clustering. *Pattern Recognition*, 41(1):191–203, 2008.
- [7] D. Dua and C. Graff. Uci machine learning repository, 2019. <http://archive.ics.uci.edu/ml>.
- [8] Martin Ester, Hans-Peter Kriegel, Jörg Sander, and Xiaowei Xu. A density-based algorithm for discovering clusters in large spatial databases with noise. In *Proceedings of the 2nd International Conference on Knowledge Discovery and Data Mining (KDD)*, pages 226–231, 1996.
- [9] Thomas S. Ferguson. A bayesian analysis of some nonparametric problems. *The Annals of Statistics*, 1(2):209–230, 1973.
- [10] P. Fränti and O. Virmajoki. Iterative shrinking method for clustering problems. *Pattern Recognition*, 39(5):761–765, 2006.
- [11] Marek Gagolewski et al. A benchmark suite for clustering algorithms: Version 1.1.0. <https://github.com/gagolews/clustering-data-v1/releases/tag/v1.1.0>, 2022. Accessed: 2025-06-26.
- [12] Charles R Harris, K Jarrod Millman, Stéfan J van der Walt, Ralf Gommers, Pauli Virtanen, David Cournapeau, Eric Wieser, Julian Taylor, Sebastian Berg, Nathaniel J Smith, et al. Array programming with NumPy. *Nature*, 585(7825):357–362, 2020.
- [13] Md. Yeamin Hossain, S. Sayed, Md. Mosaddequr Rahman, Mir Ali, Md Hossen, Abdallah Elgorban, Zoarder Ahmed, and Jun Ohtomi. Length-weight relationships of nine fish species from the tetulia river, southern bangladesh. *Journal of Applied Ichthyology*, 31, 2015.
- [14] Wei Hu, Gang Wang, and Bao-Gang Hu. Learning representations for deep clustering. In *Proceedings of the 31st Conference on Neural Information Processing Systems (NeurIPS)*, pages 1–11, 2017.
- [15] Jonathan J. Hull. A database for handwritten text recognition research. *IEEE Transactions on Pattern Analysis and Machine Intelligence*, 16(5):550–554, 1994.
- [16] A. Jain and M. Law. Data clustering: A user’s dilemma. In *Lecture Notes in Computer Science*, volume 3776, pages 1–10, 2005.
- [17] Donald B. Johnson. Efficient algorithms for shortest paths in sparse networks. *Journal of the ACM*, 24(1):1–13, 1977.
- [18] Joe H. Ward Jr. Hierarchical grouping to optimize an objective function. *Journal of the American Statistical Association*, 58(301):236–244, 1963.
- [19] J. B. MacQueen. Some methods for classification and analysis of multivariate observations. In L. M. Le Cam and J. Neyman, editors, *Proceedings of the Fifth Berkeley Symposium on Mathematical Statistics and Probability, Vol. 1*, pages 281–297. University of California Press, 1967.
- [20] Yu. A. Malkov and D. A. Yashunin. Efficient and robust approximate nearest neighbor search using hierarchical navigable small world graphs. *IEEE Transactions on Pattern Analysis and Machine Intelligence*, 42(4):824–836, 2018.
- [21] Leland McInnes, John Healy, and Sean Astels. hdbscan: Hierarchical density based clustering. *Journal of Open Source Software*, 2(11), 2017.
- [22] Geoffrey J. McLachlan and Kaye E. Basford. *Mixture Models: Inference and Applications to Clustering*. Marcel Dekker, New York, 1988.
- [23] F. Pedregosa, G. Varoquaux, A. Gramfort, V. Michel, B. Thirion, O. Grisel, M. Blondel, P. Prettenhofer, R. Weiss, V. Dubourg, J. Vanderplas, A. Passos, D. Cournapeau, M. Brucher, M. Perrot, and E. Duchesnay. Scikit-learn: Machine learning in python. *Journal of Machine Learning Research*, 12:2825–2830, 2011.
- [24] Jianbo Shi and Jitendra Malik. Normalized cuts and image segmentation. *IEEE Transactions on Pattern Analysis and Machine Intelligence*, 22(8):888–905, 2000.
- [25] Tawei. Fish species sampling data – length and weight. <https://www.kaggle.com/datasets/taweilo/fish-species-sampling-weight-and-height-data>, 2019. Kaggle dataset.
- [26] Vincent A. Traag, Ludo Waltman, and Nees Jan van Eck. From louvain to leiden: Guaranteeing well-connected communities. *Scientific Reports*, 9(1):5233, 2019.
- [27] UCI Machine Learning Repository (via Kaggle). Human activity recognition with smartphones dataset. <https://www.kaggle.com/datasets/uciml/human-activity-recognition-with-smartphones?select=train.csv>, 2019. Accessed: 2025-10-26.
- [28] Junyuan Xie, Ross Girshick, and Ali Farhadi. Unsupervised deep embedding for clustering analysis. In *Proceedings of the 33rd International Conference on Machine Learning (ICML)*, pages 478–487, 2016.
- [29] C.T. Zahn. Graph-theoretical methods for detecting and describing gestalt clusters. *IEEE Transactions on Computers*, C-20(1):68–86, 1971.

APPENDIX A EXPRESSIVE CAPACITY RESULTS

Tables IV and V show results from the Expressive Capacity experiment in Section VI.

APPENDIX B DEVELOPMENT DATASETS

- **Small Data (custom dataset):** 1D dataset of 10 points in a line. Tests algorithm behavior on very small and low-dimensional datasets.

- **Ejected Mass (custom dataset):** 2D dataset featuring a uniform mass with a few far "outlier" points, for testing "farness" heuristics.
 - **Density Gradient (custom dataset):** 2D dataset of 300 points – a Gaussian blob with a dense inner core and gradually sparser outer regions. Designed to test ability to climb density gradients.
 - **S1** [10]: S-sets benchmark dataset. A 2D dataset consisting of 5000 points in 15 Gaussian clusters. Designed to test scalability and resolution of clustering methods.
 - **Rectangle (custom dataset):** 2D dataset with points arranged along the perimeter of a rectangle. Tests shape-recognition abilities.
 - **Circles** [23]: Synthetic 2D dataset of two concentric circles. Used to test non-linear separability in clustering.
 - **Moons** [23]: Synthetic 2D dataset of two interleaving half-moon shapes. Tests non-linear separability.
 - **Jain** [16]: 373-point 2D clustering dataset, two clusters with irregular boundaries. Benchmark for clustering algorithms.
 - **Pathbased** [6]: Synthetic 2D dataset where clusters follow curved paths. Challenges density-based methods.
 - **Compound** [29]: Clustering benchmark dataset with 399 points, 6 irregularly shaped clusters. Designed to challenge Euclidean clustering methods.
 - **Fish Data** [13], [25]: Length-weight dataset of 9 fish species from the Tetulia River, Bangladesh (3 features: length, weight, width/length ratio).
- Real-world dataset*
- **Swiss Roll** [23]: Synthetic 3D manifold dataset in a rolled shape. Common in manifold learning and non-linear clustering.
 - **Iris** [7]: UCI Iris dataset (150 samples, 4 features). 3 iris species. Classic benchmark in clustering and classification.
 - **Fixed Density (custom dataset):** 6D dataset with 5 well-separated Gaussian blobs of similar density. Sanity check for moderate-dimensional clustering.
 - **Varying Density (custom dataset):** 8D dataset with 3 Gaussian blobs of different densities. Tests core functionality in an idealized scenario.
 - **Wine** [7]: UCI Wine dataset (178 samples, 13 features). Classification of wines from chemical analysis (3 classes).
 - **50D Density Gradient (custom dataset):** 50D extension of the 2D density gradient Gaussian cluster. Sanity check in high-dimensional space.

TABLE IV

GROUND-TRUTH-TUNED CLUSTERING PERFORMANCE ACROSS 2D AND 3D DATASETS (MEAN \pm 1 SD; ARI ON TOP, NMI IN THE MIDDLE, RUNTIME ON THE BOTTOM). STANDARD DEVIATIONS BELOW 0.005 ARE OMITTED. BOLD INDICATES THE BEST PER ROW. DEVELOPMENT DATASETS ARE MARKED WITH *.

Dataset (N, D)	EVINGCA	HDBSCAN	K-means	GMM	Spectral
Compound* (399, 2)	0.94	0.85	0.55 \pm 0.06	0.6 \pm 0.07	0.49
	0.95	0.86	0.71 \pm 0.04	0.78 \pm 0.04	0.75
	0.03 s	<0.01 s	0.02 \pm 0.02 s	0.01 s	0.1 \pm 0.01 s
Spiral (312, 2)	1.0	1.0	-0.01	0.02 \pm 0.01	0.8
	1.0	1.0	0.0	0.04 \pm 0.02	0.78
	0.02 s	<0.01 s	0.01 s	0.01 \pm 0.02 s	0.11 \pm 0.01 s
Nested Circles (900, 2)	1.0	0.83	-0.0	0.08 \pm 0.05	1.0
	1.0	0.86	0.0	0.1 \pm 0.05	1.0
	0.04 s	0.01 s	0.01 s	0.01 \pm 0.01 s	0.2 \pm 0.02 s
Smile (1000, 2)	1.0	1.0	0.52 \pm 0.07	0.65 \pm 0.15	0.32 \pm 0.08
	1.0	1.0	0.77 \pm 0.03	0.83 \pm 0.06	0.66 \pm 0.05
	0.04 s	0.01 s	0.01 s	0.02 s	0.14 \pm 0.01 s
D31 (3100, 2)	0.92	0.61	0.92 \pm 0.02	0.92 \pm 0.02	0.95
	0.95	0.85	0.96 \pm 0.01	0.96	0.97
	0.23 \pm 0.02 s	0.03 s	0.01 s	0.55 \pm 0.07 s	0.4 \pm 0.03 s
Flame (240, 2)	0.98	0.76	0.49 \pm 0.03	0.17 \pm 0.17	0.93
	0.96	0.69	0.44 \pm 0.03	0.29 \pm 0.11	0.89
	0.02 s	<0.01 s	0.01 s	0.01 s	0.1 \pm 0.01 s
Labirynt (3546, 2)	0.76	0.55	0.3 \pm 0.02	0.55 \pm 0.09	0.72
	0.85	0.75	0.52 \pm 0.02	0.73 \pm 0.07	0.87
	0.2 s	0.04 s	0.01 s	0.45 \pm 0.06 s	0.54 \pm 0.02 s
Trapped Lovers (5000, 3)	1.0	1.0	0.15	0.87 \pm 0.26	1.0
	1.0	1.0	0.38	0.92 \pm 0.16	1.0
	0.16 s	0.09 s	0.01 s	0.11 \pm 0.02 s	1.07 \pm 0.04 s
Fish* (4080, 3)	0.8	0.86	0.81	0.84	0.75 \pm 0.09
	0.92	0.94	0.91	0.94	0.91 \pm 0.03
	0.13 \pm 0.01 s	0.06 s	0.01 s	0.07 s	0.51 \pm 0.08 s
MK3 (600, 3)	0.8	0.57	0.89	0.87	0.88
	0.8	0.72	0.86	0.85	0.85
	0.03 s	0.01 s	0.01 s	0.01 s	0.15 \pm 0.01 s
Tetra (400, 3)	1.0	0.8	1.0	1.0	1.0
	1.0	0.81	1.0	1.0	1.0
	0.02 s	0.01 s	0.01 s	0.01 s	0.12 \pm 0.01 s

TABLE V

GROUND-TRUTH-TUNED CLUSTERING PERFORMANCE ACROSS 4D+ DATASETS (MEAN \pm 1 SD; ARI ON TOP, NMI IN THE MIDDLE, RUNTIME ON THE BOTTOM). STANDARD DEVIATIONS BELOW 0.005 ARE OMITTED. BOLD INDICATES THE BEST PER ROW. DEVELOPMENT DATASETS ARE MARKED WITH *.

Dataset (N, D)	EVINGCA	HDBSCAN	K-means	GMM	Spectral
Iris* (150, 4)	0.9	0.57	0.71 \pm 0.01	0.9	0.74
	0.89	0.73	0.72 \pm 0.01	0.9	0.78
	0.02 s	<0.01 s	0.01 s	0.05 \pm 0.02 s	0.1 \pm 0.01 s
Banknote (1372, 4)	0.97	0.55	0.02	0.11	0.44
	0.94	0.54	0.02	0.13	0.38
	0.05 s	0.02 s	0.01 s	0.02 s	0.25 \pm 0.02 s
Ecoli (336, 7)	0.72	0.44	0.43 \pm 0.05	0.62 \pm 0.01	0.39
	0.69	0.45	0.59 \pm 0.03	0.6 \pm 0.01	0.58
	0.02 s	0.01 s	0.01 s	0.16 \pm 0.09 s	0.12 \pm 0.01 s
Seeds (210, 7)	0.63	0.26	0.7 \pm 0.01	0.7	0.73
	0.65	0.38	0.67	0.67	0.72
	0.02 s	<0.01 s	0.01 s	0.01 s	0.11 \pm 0.01 s
Wine* (178, 13)	0.88	0.34	0.85 \pm 0.02	0.85 \pm 0.08	0.9
	0.86	0.43	0.83 \pm 0.02	0.84 \pm 0.06	0.88
	0.02 s	<0.01 s	0.01 s	0.07 \pm 0.05 s	0.09 s
Pendigits (10000, 16)	0.78	0.54	0.55 \pm 0.04	0.55 \pm 0.03	0.74
	0.84	0.73	0.68 \pm 0.01	0.7 \pm 0.02	0.82
	0.39 \pm 0.03 s	1.08 \pm 0.01 s	0.02 s	0.45 \pm 0.05 s	4.06 \pm 0.06 s
Statlog (2310, 19)	0.58	0.43	0.49 \pm 0.02	0.52 \pm 0.01	0.57
	0.69	0.63	0.61	0.64	0.68
	0.11 \pm 0.01 s	0.15 s	0.01 s	0.07 \pm 0.01 s	0.41 \pm 0.03 s
WDBC (569, 30)	0.75	0.25	0.73	0.68	0.81
	0.69	0.25	0.62	0.56	0.73
	0.05 s	0.02 s	0.01 s	0.01 s	0.09 \pm 0.01 s
Digits (1797, 64)	0.87	0.4	0.64 \pm 0.04	0.64 \pm 0.02	0.81
	0.9	0.7	0.74 \pm 0.02	0.74 \pm 0.01	0.9
	0.08 s	0.16 s	0.01 s	0.14 \pm 0.01 s	0.29 \pm 0.03 s
G2mg_128_20 (2048, 128)	0.99	0.0	1.0	1.0	1.0
	0.97	0.08	1.0	1.0	0.99
	0.2 s	0.4 \pm 0.01 s	0.01 s	0.07 s	0.57 \pm 0.03 s
G2mg_128_30 (2048, 128)	0.08	0.0	0.95	0.95	0.93
	0.1	0.01	0.9	0.9	0.88
	0.12 s	0.41 \pm 0.01 s	0.01 s	0.09 \pm 0.01 s	0.86 \pm 0.02 s
USPS (9298, 256)	0.61	0.11	0.53 \pm 0.02	0.0	0.65
	0.74	0.43	0.62 \pm 0.01	0.0	0.8
	0.74 \pm 0.02 s	16.29 \pm 0.17 s	0.09 \pm 0.01 s	0.22 \pm 0.01 s	4.11 \pm 0.07 s
HAR Train Subset (7352, 562)	0.52	0.22	0.47 \pm 0.05	0.31 \pm 0.06	0.57
	0.68	0.35	0.61 \pm 0.03	0.47 \pm 0.05	0.69
	0.76 \pm 0.02 s	25.6 \pm 0.19 s	0.12 \pm 0.02 s	78.83 \pm 16.01 s	4.64 \pm 0.1 s
Fashion-MNIST (10000, 784)	0.38	0.02	0.38 \pm 0.02	0.0	0.41
	0.59	0.06	0.53 \pm 0.01	0.0	0.6
	2.1 \pm 0.05 s	62.55 \pm 0.66 s	0.3 \pm 0.1 s	0.86 \pm 0.01 s	3.61 \pm 0.09 s
20 Newsgroups (10000, 2000)	0.0	-0.0	0.02 \pm 0.01	0.0	0.0
	0.05	0.01	0.07 \pm 0.03	0.0	0.06
	2.64 \pm 0.14 s	159.4 s	1.08 \pm 0.38 s	4.56 \pm 0.08 s	3.78 \pm 0.06 s

TABLE VI

EXPRESSIVE CAPACITY ABLATION: MEAN ARI (\pm STD) ACROSS DATASETS AND ABLATIONS. BOLD INDICATES THE BEST VALUE PER ROW. STANDARD DEVIATIONS BELOW 0.005 ARE OMITTED.